Energy xxx (2014) 1–14

Contents lists available at ScienceDirect

Energy

journal homepage: www.elsevier.com/locate/energy

Exergy analysis and annual exergetic performance evaluation of solar hybrid STIG (steam injected gas turbine) cycle for Indian conditions

A. Immanuel Selwynraj [a], S. Iniyan [a, *], Guy Polonsky [c], L. Suganthi [b], Abraham Kribus [c]

[a] Dept. of Mechanical Engineering, Anna University, Chennai 600 025, India
[b] Dept. of Management Studies, Anna University, Chennai 600 025, India
[c] School of Mechanical Engineering, Tel Aviv University, Tel Aviv 6997801, Israel

ARTICLE INFO

Article history:
Received 22 August 2014
Received in revised form
28 November 2014
Accepted 1 December 2014
Available online xxx

Keywords:
Solar STIG cycle
Steam injection
Exergetic performance
Gas turbine

ABSTRACT

The STIG (steam injected gas turbine) cycle offers a way for increasing the power, efficiency and NO_x reduction in gas turbines by injecting steam into the combustor. The present exergetic study is to investigate the influence of compressor PR (pressure ratio), TIT (turbine inlet temperature) and SAR (steam to air ratio) on the solar hybrid STIG cycle. Exergy analysis was performed for four cases based on the parameters of real gas turbines. Annual exergetic performance is also presented for the sites Indore and Jaipur in India under constant and variable power modes. The analysis suggests that the steam injection does not affect the performance of compressor. The total exergy destruction in the cycle increases with SAR and TIT. The exergetic efficiency also increases in the range of 40%–54.2% with SAR up to 0.9. The magnitude of exergy destruction in all components in the cycle (except compressor) increases by increasing SAR. Nevertheless, largest component of exergy destruction in the combustion chamber increases with SAR and TIT about 53% at SAR 0.9. The exergetic efficiency of combustor increases from 74.5% to 81.8% with increasing SAR from 0.3 to 0.9. The exergy destruction in the turbine increases considerably with compressor pressure ratio, sparingly with SAR and independent of TIT. The exergy destruction in the SH (super heater) is less compared to the economiser in the HRSG (heat recovery steam generator). The contribution of solar energy (exergetic solar fraction) is more sensitive to TIT and SAR than PR. It is noticed that increase in turbine outlet temperature, led by PR and TIT, decreases the exergetic solar fraction, and the cycle exergetic efficiency improves as the exergetic solar fraction increases, which leads to an improved performance device. The second largest percentage of exergy destruction is in the flue gas condenser to recover water for recycling, and the heat removed from the condenser is lost to the surroundings by cooling air. The annual values of exergetic solar fraction and exergetic efficiency at Indore are higher than Jaipur in both constant and variable power modes of operation.

1. Introduction

Electric power generation, in India, is an important issue today and is the backbone of economic development of the country. In many parts of the world, gas turbines with new technologies are being used at peak and base load power plants to meet the rapidly growing energy demand. Power production from solar energy is intermittent and high cost of solar thermal systems makes sense only in regions with high solar insolation. The idea of a hybrid system is to provide higher availability of the plant by allowing stable operation even in periods of low irradiation, which also translates into better financial conditions for the plant. In regions of lower solar availability, hybrid systems could help in making use of the available solar radiation by providing stable operation conditions and reducing fossil fuel consumption. Steam injection concept has been practiced since 1980's for power augmentation, NO_x, CO_2 reduction and to cool the blades more effectively than air. The aero derivative gas turbines for power generation are being used with minor modifications to operate the STIG (steam injected gas turbine) as base load plant.

M. Livshits and A. Kribus [1] described that in the conventional STIG, the flow rate of steam is limited by the amount of thermal energy available at the HRSG (heat recovery steam generator) from

* Corresponding author.
E-mail address: iniyan777@hotmail.com (S. Iniyan).

http://dx.doi.org/10.1016/j.energy.2014.12.001
0360-5442/

the turbine exhaust stream. If an additional heat source is available, then larger amounts of steam could be injected into the cycle. In the solar STIG cycle, the additional steam is provided from solar concentrating collectors, producing a hybrid cycle with heat input from both solar collectors and from fuel in the combustor (Fig. 1). Solar heat is used mainly for evaporation. Recuperation of gas turbine waste heat is assigned primarily for super heater and economizer, to avoid the thermodynamic irreversibility and loss of work potential due to large temperature differences. The solar steam for the hybrid STIG cycle should match the turbine pressure, typically in the range of 10–30 bar, corresponding to saturated steam temperatures of 180–234 °C. These pressures and temperatures are lower than those of current solar power plants and can be easily achieved with lower cost versions of linear concentrators such as parabolic trough and linear Fresnel collectors.

Exergetic analysis is a qualitative thermodynamic assessment of any power generation system. In the last several decades, exergy analysis has begun to be used for system optimization. The method of exergy analysis (availability analysis) based on the second law of thermodynamics enables the location, cause, and true magnitude of energy resource waste and loss to be determined and also provides component efficiency. Such information can be used in the design of new energy efficient systems and for improving the performance of existing systems. Exergy analysis also provides insights that eludes a purely first law approach [2]. Therefore, it is essential to study the solar STIG cycle based on the second law analysis of thermodynamics. The exergy analysis is applied here to the thermodynamic cycle excluding the solar collector field.

Many researchers have performed the exergetic analysis of fossil fuel and renewable energy based power generation systems. The outcomes of second law based analysis of gas turbine plant, generally pertaining to steam injected gas turbine components are recapitulated in this section. M. Jonssona and J. Yan [3] summarized the description of available commercial steam injected gas turbines and highlighted the research and development in the modified steam injected gas turbine cycles including intercoolers, recuperators, reheat or topping steam turbines and cogeneration investigated by many researchers. D. P. S Abam and N. N. Moses [4] investigated the second law efficiencies of the 33 MW gas turbine plant and the combustion chamber are found to decrease more significantly with increase in the ambient temperature than the air compressor and the gas turbine. Yaser Sahebi and Hasan Athari [5] studied the irreversibility of compressor, combustion chamber and turbine decreases in the gas turbine cycle with steam injection and inlet fogging cooler and compared that the second law efficiency of STIG cycle is more than both the simple gas turbine cycle and steam injected gas turbine with inlet fogging cooler at 45 °C ambient temperature and 15% relative humidity. R. Layi Fagbenle et al. [6] indicated that the exergy loss in the combustion chamber is largest at about 79% of the total system exergy loss and the exergy defect associated with the steam injection is only 1.3% of the total exergy loss, and is not excessive for the 53 MW (net) biogas fired integrated gasification steam injected gas turbine (BIG (biomass integrated gasification)/STIG) plant based on the LM 5000 aero derivative gas turbine.

F.J. Wang and J.S. Chiou [7] analysed a retrofitted simple cycle GENSET (cogeneration) with GE Frame 6B and presented that the exergy efficiency of combustor is 76% which is higher than that of HRSG about 62%. Besides, the power output of STIG cycle is less sensitive to ambient temperature than that of a simple cycle. They also studied the STIG with inlet air cooling using Taipower's Frame 7B simple cycle GENSET that the effect of the STIG is more profound than that of the IAC (inlet air cooling) in improving the power output and efficiency. The exergy loss per MW output, the system with both the STIG and IAC feature is 23.7% lower than that of the basic system [8]. T. Srinivas et al. [9] investigated that the major percentage of exergetic loss that occurs in combustion chamber decreases from 38.5% (without steam injection) to 37.4% (3 kg steam/kg fuel) with introduction of steam injection into the combustion chamber for a STIG based combined cycle. Mustafa Zeki Yilmazoglu et al. [10] examined the effect of steam injection mass flow rate, duct burner exhaust temperature on the combined cycle power plant in Turkey using GE7251FB model gas turbine-generator with 373 MW electrical power (in ISO conditions), CMI model heat recovery steam generator and ALSTOM steam turbine generator with 92.26 MW electrical power, and found that the duct burner exit temperature and steam injection mass flow rate to the combustion chamber decreases the exergy efficiency from 50.52 to 50.02% due to additional fuel consumption and a bled steam from HP turbine is injected into the combustion chamber to improve the net power and minimize the NO_x emissions of the power plant. Sadegh Motahar and Ali Akbar Alemrajabi [11] evaluated that the overall exergetic efficiency calculated for the base solid oxide fuel cell and steam injected gas turbine hybrid power system is 58.28% and steam injection boosts the exergetic efficiency by 12.11%.

K. Nishida et al. [12] analysed that the exergy efficiency of the regenerative STIG with steam injection after the compressor is higher than that of the simple, regenerative gas turbine cycle, regenerative cycle with water injection before and after compressor, STIG and regenerative STIG with steam injection into

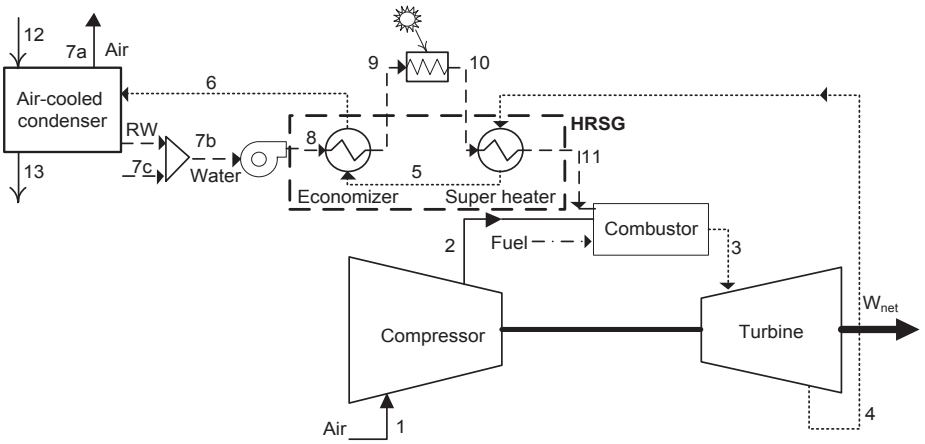

Fig. 1. Layout of the solar hybrid STIG cycle.

Please cite this article in press as: Selwynraj AI, et al., Exergy analysis and annual exergetic performance evaluation of solar hybrid STIG (steam injected gas turbine) cycle for Indian conditions, Energy (2014), http://dx.doi.org/10.1016/j.energy.2014.12.001

the combustor. They also investigated that the exergy recovered in the heat exchanger of the regenerative STIG with steam injection after the compressor is larger than that of the regenerative STIG with steam injection into the combustor, because the exhaust heat from a gas turbine is recovered by both the compressed air and steam. M. Tajik Mansouri et al. [13] investigated the effect of HRSG pressure levels on exergy efficiency of gas turbine combined cycle power plants and showed that increase in pressure levels of steam generation at HRSG leads to an increase in heat recovery from the flue gas (in HRSG) and thereby decreases the exergy destruction due to heat transfer in HRSG and as a result, the exergy efficiency of HRSG and combined cycle power plant increases respectively. S.C. Kaushik et al. [14] compared the energy and exergy analyses of existing coal and gas fired thermal power plants in order to identify the needed improvement and also mentioned that efficiency of heat exchanger is improved by increasing the heat transfer area which involves extra cost.

Pouria Ahmadi et al. [15] investigated the effect of supplementary firing on the performance of the natural gas fired combined cycle power plant that increasing the degree of supplementary firing reduces the combined cycle power plant exergy efficiency due to the subsequent increase in the exergy destruction in the duct burner and HRSG. F. Guarinello Jr. et al. [16] observed that the maximum exergetic efficiency of the system occurs when there is no supplementary burning and the cost of electricity is lower in the STIG condition. V. Siva Reddy et al. [17] carried out the exergetic analysis of parabolic trough concentrating solar thermal power plant, concluded that the over all year round operation of Jodhpur location is found to be better as compared to Delhi. Numerous researchers have studied the exergetic performance of gas fired plants and confirmed that the main component of irreversibility is combustion chamber. Moreover, to enhance the exergy recovered, the pinch point should be minimum in HRSG.

M. Livshits and A. Kribus [1] analysed the nominal energy performance of solar hybrid steam injection gas turbine cycle for varying pressure ratio and turbine inlet temperature using Honeywell Unisim process simulation software. Preliminary annual thermodynamic analyses were reported for the climatic conditions at sites in Israel by M. Livshits and A. Kribus [18] and in India by A.I. Selwynraj et al. [19]. The exergetic performance of this cycle has not been investigated so far. The objective of this study is to evaluate the exergetic performance of the solar hybrid STIG cycle over a wide range of operating parameters (PR (pressure ratio), TIT (turbine inlet temperature) and SAR (steam to air ratio)) to pinpoint and quantify the imperfections of each component in the cycle. The annual exergetic performance is also analysed for two sites in India with detailed information on local climatic conditions in order to assess the daily effect on inefficiencies and thereby help to improve the performance of the cycle.

2. Process description of solar STIG cycle

Air drawn from the atmosphere is compressed (1–2) as shown in Fig. 1. In parallel, the recovered water from the condenser at atmospheric pressure is pumped (7b–8) with pressure matching the compressor outlet and then heated in the economizer (8–9). After recovering the low temperature heat from the exhaust gas at the super heater exit (5) is used for preheating the pressurized water in the economizer is then allowed to condense the water vapour present in the flue gas (6) by air cooled condenser. The preheated water absorbs latent heat of evaporation from the low temperature (up to 250 °C) solar collectors (9–10). The saturated steam from the solar field is super heated (10–11) by turbine exhaust gas (4). The compressed air (2) is fed to the combustor, and superheated steam (11) is also injected into the combustor together with required fuel. The combustion products along with injected steam elevated to required TIT are expanded through the turbine (3–4) which produces work. The thermal energy available in the turbine exhaust is primarily used by super heater (4–5) and then economizer (5–6). The condenser recovered water vapour from the flue gas (6) is recycled back to the pump (7b) and the low temperature flue gas (7a) is expelled to the atmosphere through stack. The atmospheric air supplied by condenser fans removes the heat from flue gas and then goes off to the surroundings (12–13).

3. Simulation methodology

A detailed thermodynamic simulation of the solar hybrid cycle shown in Fig. 1 was carried out using Honeywell Unisim process simulation software, and the cycle components were represented by using standard library component models. The mass flow rate of air through the compressor was fixed as 1 kg/s.

Steam injection into combustor increases the power output of a gas turbine by increasing the mass flow of 1 + f + SAR kg/s through the turbine, relative to the compressor, without significantly increasing the power required to drive the compressor. With steam addition the turbine flow is increased resulting in greater power output. The air inlet to compressor is defined according to ISO conditions (1.013 bar, 15 °C and 60% RH) for the nominal performance simulation. The dT value is 10 °C based on the local climatic conditions for the sites considered in this analysis. The values of input parameters used in the simulation are presented in Table 1.

Simulations were performed for varying the compressor pressure ratio (PR = 10–30), the turbine inlet temperature (TIT = 900 °C–1400 °C) and steam to air ratio (SAR = 0.3–1.2). The amount of steam injected into the cycle was varied over a wide range, while the mass flow rate of the air was kept fixed. During this variation, the compressor sizing and performance are fixed, but the sizes of the turbine and the heat exchangers are assumed to adapt as needed to accommodate the higher mass flow rate. The annual thermodynamic simulations were carried out based on the availability of solar radiation and ambient conditions (Dry bulb temperature, Relative humidity) for two sites in India under constant power, keeping the amount of injected steam constant regardless of the solar conditions by using duct firing, and variable power, where the steam flow rate is allowed to vary in correspondence to the availability of solar heat, scenarios for the case B mentioned in Table 2. The simulations provided the temperatures, pressures, flow rates, enthalpy, entropy and composition at each point in the cycle, as well as energy balances for each component in the cycle. Exergy analysis was performed for four cases defined, based on the parameters of real turbines in Table 2, and annual exergetic analysis was also carried out for two sites in India: Jaipur (annual DNI (direct normal irradiance) = 2180 kWh/m^{2}yr) and Indore (annual DNI = 2061 kWh/m^{2}yr). Hourly meteorological data for a typical year was derived from the Meteonorm software for each site. The climatic data includes ambient air temperature, relative humidity and DNI. Annual values were obtained by summation of all

Table 1
Input to the component models used in the simulation.

Parameter	Value
Turbine isentropic efficiency	90%
Compressor isentropic efficiency	85%
Water pump isentropic efficiency	80%
Pressure drop in heat exchangers (except condenser)	3%
Pressure drop in combustor	4%
Minimum approach for the HRSG	10 °C
Stack temperature (T_{7a})	Max (T_0+dT,40 °C)

Please cite this article in press as: Selwynraj AI, et al., Exergy analysis and annual exergetic performance evaluation of solar hybrid STIG (steam injected gas turbine) cycle for Indian conditions, Energy (2014), http://dx.doi.org/10.1016/j.energy.2014.12.001

Table 2
The real gas turbines and its operational parameters for the four cases used in the simulations [1].

Case	Real gas turbine	PR	TIT, °C
A	Solar Centaur 40-T4700	10	900
B	GE LM2000	15	1100
C	GE LM6000 PC	30	1200
D	Mitsubishi 701G	20	1400

representative days, weighted by number of days in each month and a clearness index for the month. The operating days were considered only the days with at least 3 h of DNI higher than 300 W/m^2. In each month, operation hours were calculated as hours when the plant's incremental efficiency is positive and the hourly DNI is higher than 300 W/m^2 [20]. The annual variation of DNI for Jaipur and Indore are shown in Fig. 2. Though Jaipur has higher DNI, the DNI distribution in Indore is comparatively more uniform than Jaipur. Generally, many parts of India have lower DNI during the months of June to August due to summer monsoons. Highest DNI values are recorded during beginning and end of the year.

The variations of ambient temperature are very similar in both locations of Indore and Jaipur are shown in Fig 3. The environment air temperature affects the compressor and condenser performance in the solar STIG cycle.

The ambient temperature is higher during summer months having low insolations and lower during beginning and end of the year having higher DNI values. The months having higher DNI with lower ambient temperature is the most favourable conditions for solar STIG plant which yields better performance.

4. Exergy analysis

Exergy is defined as the maximum amount of work which can be produced by a system or a flow of matter or energy as it comes to equilibrium with a reference environment. Due to the irreversibility of thermal processes, the work obtained is always less than the maximum work. Hence, by analysing work loss within a system, imperfections can be quantified, and possible improvements suggested. If the effects of kinetic and potential are ignored, the specific exergy of a system consists of physical exergy and chemical exergy can be expressed as,

$$e_{sys} = e^{ph} + e^{ch} \tag{1}$$

Physical exergy is the work obtainable by taking the system through reversible physical process – compression, expansion and heat exchanging to the temperature and pressure of the environment. Physical flow exergy for simple compressible pure substances is given as,

$$e^{ph} = [(h - h_0) - T_0(s - s_0)] \tag{2}$$

Chemical exergy is the maximum useful energy which would be attained by passing from the environmental state to the dead state, by means of chemical processes with reactants and products at the environmental temperature and pressure, when the stream composition is not in chemical equilibrium with the environment. The fuel is assumed to be methane, the main component in natural gas. The reaction heat is evaluated using the stoichiometric proportions for the combustion reaction,

$$CH_4 + 2O_2 \rightarrow CO_2 + 2H_2O$$

The accurate relation for chemical exergy of that fuel can be defined as,

$$\begin{aligned}\overline{e}^{ch} = &\left[\overline{h}_{CH_4} + 2\overline{h}_{O_2} - \overline{h}_{CO_2} - 2\overline{h}_{H_2O}\right]_{(T_0,P_0)} \\ &- T_0\left[\overline{s}_{CH_4} + 2\overline{s}_{O_2} - \overline{s}_{CO_2} - 2\overline{s}_{H_2O}\right]_{(T_0,P_0)} \\ &+ \overline{R}T_0 ln\left(\frac{x_{O_2}^2}{x_{CO_2}.x_{H_2O}^2}\right)\end{aligned} \tag{3}$$

Exergy can be transferred by work, heat and mass flow. The exergy content of a rate of work transfer is,

$$\dot{E}_W = \dot{W} \tag{4}$$

The exergy content of a heat transfer rate $\dot{Q}$ at a temperature T is,

$$\dot{E}_Q = \left(1 - \frac{T_0}{T}\right)\dot{Q} \tag{5}$$

The exergy rate of mass flow is,

$$\dot{E}_m = \dot{m}\left[(h - h_0) - T_0(s - s_0) + \frac{C^2}{2} + gZ\right] \tag{6}$$

Exergy destruction or irreversibility is the exergy destroyed due to friction, mixing, chemical reactions, heat transfer through a finite temperature difference, unrestrained expansion, non-quasi-equilibrium compression or expansion and anything that cause

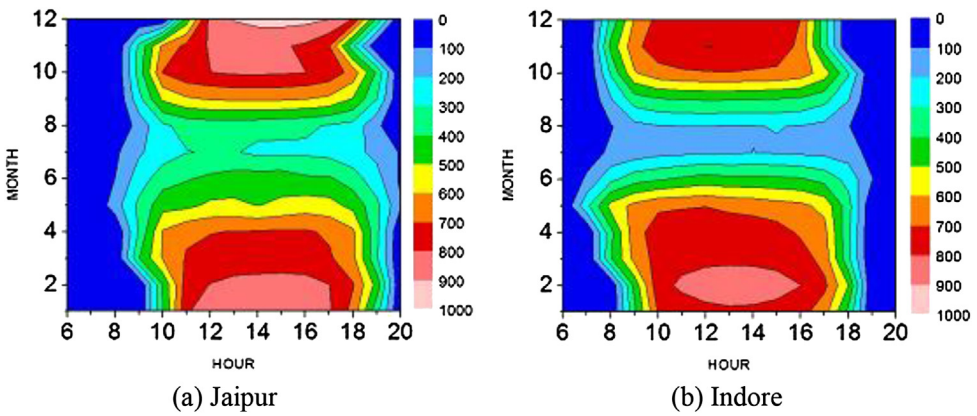

Fig. 2. Annual variation of DNI in W/m^2 for Jaipur and Indore.

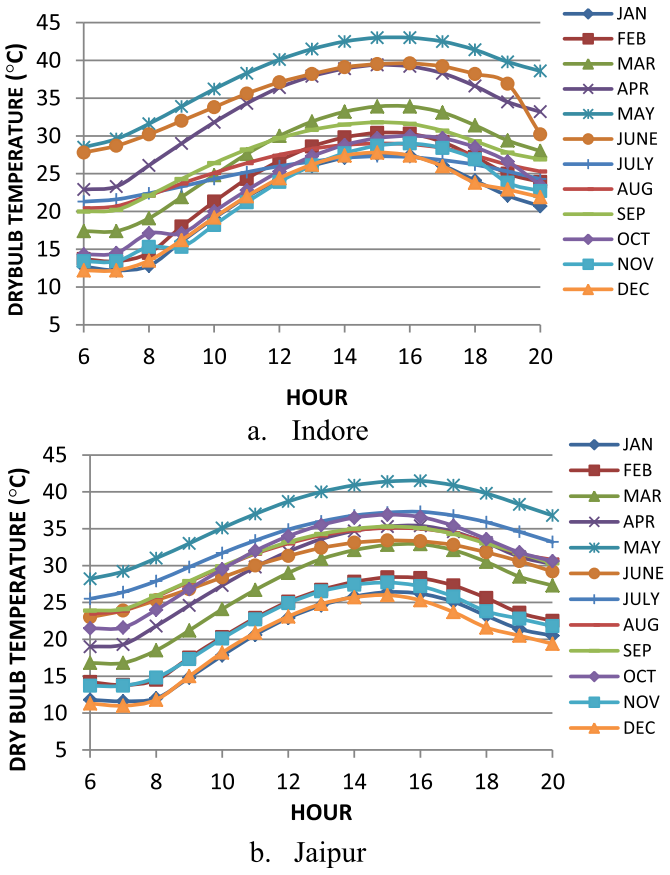

Fig. 3. Annual dry bulb temperature variation for Indore and Jaipur.

entropy generation. The exergy destruction in the overall system is equal to the sum of exergy destructions in all the components in the system. Exergy loss is the transfer of exergy from the overall system to its surroundings. The exergy balance is a statement of the law of degradation of energy. The exergy balance equation for the steady state devices is given as,

$$\dot{E}_Q - \dot{E}_W + \dot{E}_{in} - \dot{E}_{out} - \dot{E}_D = 0 \tag{7}$$

The exergy delivered by solar collector at temperature T_{10} (Temperature at Solar evaporator exit) is given by S.K.Tyagi et al. [21],

$$\dot{E}_{solar} = \left(1 - \frac{T_0}{T_{10}}\right)\dot{Q}_{solar} \tag{8}$$

Exergetic solar fraction is the ratio of input exergy contributed by solar collector system to the total exergy (fuel and solar) supplied to the cycle.

$$SF_{II} = \frac{\dot{E}_{solar}}{\dot{E}_{fuel} + \dot{E}_{solar}} \tag{9}$$

The exergetic efficiency (second law efficiency) provides a true measure of the performance of a system from the thermodynamic viewpoint. Exergetic efficiencies can be used to assess the thermodynamic performance of a component and overall plant. The exergetic efficiency of solar hybrid STIG cycle is,

$$\eta_{II} = \frac{Exergy\ Recovered}{Exergy\ supplied} = \frac{\dot{W}_N}{\dot{E}_{fuel} + \dot{E}_{solar}} \tag{10}$$

Table 3
Expressions for exergy destruction rate, exergy loss and exergetic efficiency of solar STIG cycle main components.

Plant component	Exergy destruction	Exergetic efficiency
Compressor	$\dot{E}_1 - \dot{E}_2 + \dot{W}_C$	$\frac{\dot{E}_2 - \dot{E}_1}{\dot{W}_C}$
Combustor	$\dot{E}_2 + \dot{E}_{fuel} + \dot{E}_{11} - \dot{E}_3$	$\frac{\dot{E}_3}{\dot{E}_2 + \dot{E}_{fuel} + \dot{E}_{11}}$
Turbine	$\dot{E}_3 - \dot{E}_4 - \dot{W}_T$	$\frac{\dot{W}_T}{\dot{E}_3 - \dot{E}_4}$
Super heater (SH)	$\dot{E}_4 - \dot{E}_5 + \dot{E}_{10} - \dot{E}_{11}$	$\frac{\dot{E} + \dot{E}_{11}}{\dot{E}_4 + \dot{E}_{10}}$
Economiser	$\dot{E}_5 - \dot{E}_6 + \dot{E}_8 - \dot{E}_9$	$\frac{\dot{E}_6 + \dot{E}_9}{\dot{E}_5 + \dot{E}_8}$
HRSG (SH + ECO)	$\dot{E}_4 - \dot{E}_6 + \dot{E}_8 - \dot{E}_9 + \dot{E}_{10} - \dot{E}_{11}$	$\dot{E}_6 + \frac{\dot{E}_9 + \dot{E}_{11}}{\dot{E}_4 + \dot{E}_8 + \dot{E}_{10}}$
Solar evaporator	$\dot{E}_9 + \dot{E}_{solar} - \dot{E}_{10}$	$\frac{\dot{E}_{10}}{\dot{E}_9 + \dot{E}_{solar}}$
Condenser	$\dot{E}_6 - \dot{E}_{7a} - \dot{E}_{RW} + \dot{W}_D$	$\frac{\dot{E}_{7a} + \dot{E}_{RW}}{\dot{E}_6 + \dot{W}_D}$
Pump	$\dot{E}_{7b} - \dot{E}_8 + \dot{W}_p$	$\frac{\dot{E}_8 - \dot{E}_{7b}}{\dot{W}_p}$
Stack (Wasted exergy)	$\dot{E}_{7a}$	–
Solar STIG cycle	$\dot{E}_1 + \dot{E}_{fuel} + \dot{E}_{solar} - \dot{E}_{7a} - \dot{W}_N$	$\frac{\dot{W}_N}{\dot{E}_1 + \dot{E}_{fuel} + \dot{E}_{solar}}$
Exergy loss		
Stack exhaust gas	$\left(1 - \frac{T_0}{T_{7a}}\right)\dot{Q}_{stack}$	–
Condenser cooling air	$\left(1 - \frac{T_0}{T_{13}}\right)\dot{Q}_D$	–

The net specific work in kJ/kg-air is calculated based on normalized flow rate from the specific work of the components that is obtained from the simulation,

$$\dot{W}_N = \dot{W}_T - \dot{W}_C - \dot{W}_P - \dot{W}_D \tag{11}$$

W_T is the specific work output of the turbine; and W_C, W_P and W_D are the specific work inputs of the compressor, water pump and condenser fan respectively. This is equivalent to kW per kg-air/s.

The condenser fan power consumption that was obtained from published data by M. De Paepe and E. Dick [22].

$$\dot{W}_D = \frac{0.558\dot{Q}_D}{(T_{13} - T_{12})} = \frac{0.558\dot{Q}_D}{0.755(T_6 - T_{12})} \tag{12}$$

The expressions of exergy destruction rate, exergy loss, exergetic efficiency of each component and for the overall solar STIG cycle (see Fig. 1) are shown in Table 3.

5. Results and discussions

Exergy analysis was performed using Honeywell Unisim process simulation software, in order to assess the systems thermodynamically. The results from the Table 4 show that the effect of variations of pressure ratio, turbine inlet temperature, steam to air ratio on exergy destruction in each component of solar STIG cycle, exergy loss and exergy supply from both fuel and solar energy. It is observed that the magnitude of both fuel and solar exergy input improve as SAR is increased. This is because the quantity of super heated steam being injected into the combustor is to be raised to the required TIT. At a given pressure ratio, a lower TIT will demand more solar exergy than a higher TIT. On the other hand, at a given TIT, a higher pressure ratio will lead to more solar share and reduction in fuel consumption. Because, up to SAR = 0.5, at high PR, the compressed air has more exergy while the improved solar fraction is due to the lower turbine outlet temperature caused by the higher expansion ratio. In the case of SAR = 0.3, at PR = 10 & TIT = 1200 °C, due to lower expansion ratio, the heat available from the higher turbine outlet temperature flue gas is alone sufficient to generate super heated steam. The percentage of exergy destruction,

Please cite this article in press as: Selwynraj AI, et al., Exergy analysis and annual exergetic performance evaluation of solar hybrid STIG (steam injected gas turbine) cycle for Indian conditions, Energy (2014), http://dx.doi.org/10.1016/j.energy.2014.12.001

Table 4
Results of exergy destruction, exergy loss for solar STIG cycle components and exergy supply (various PR, TIT and SAR).

Component exergy destruction (kW)	SAR = 0.3				SAR = 0.5				SAR = 0.7				SAR = 0.9			
	TIT = 900 °C		TIT = 1200 °C		TIT = 900 °C		TIT = 1200 °C		TIT = 900 °C		TIT = 1200 °C		TIT = 900 °C		TIT = 1200 °C	
	PR 10	PR 30	PR 10	PR 30	PR 10	PR 30	PR 10	PR 30	PR 10	PR 30	PR 10	PR 30	PR 10	PR 30	PR 10	PR 30
Compressor	24.07	31.18	24.07	31.18	24.07	31.18	24.07	31.18	24.07	31.18	24.07	31.18	24.07	31.18	24.07	30.12
Combustor	438.11	376.46	544.63	480.78	522.22	491.55	627.79	593.84	598.94	597.85	703.07	696.52	671.04	698.29	772.24	789.60
Turbine	34.56	59.15	34.52	58.72	41.76	71.37	41.67	70.78	48.96	83.59	48.82	82.85	56.16	95.83	55.97	94.93
Super heater (SH)	20.01	6.83	36.86	16.51	28.44	9.68	54.32	24.23	35.90	12.39	69.02	30.87	42.51	15.06	81.92	36.74
Economiser (ECO)	50.46	19.54	116.12	43.07	48.61	21.00	108.88	41.20	54.64	34.51	110.93	53.02	60.97	46.36	113.98	64.69
HRSG (SH + ECO)	70.46	26.38	152.98	59.58	77.05	30.68	163.20	65.43	90.55	46.90	179.95	83.89	103.48	61.41	195.91	101.43
Solar evaporator	0.57	0.12	1.16	0.57	0.47	0.01	1.09	0.48	0.30	0.01	0.93	0.28	0.12	1.08	0.77	0.08
Condenser	124.99	123.62	136.99	136.15	211.45	210.08	224.78	224.46	308.44	308.84	324.10	325.97	408.16	410.32	425.78	430.27
Stack (Wasted exergy)	5.69	5.72	5.59	5.61	5.65	5.66	5.54	5.54	5.61	5.61	5.49	5.47	5.57	5.56	5.44	5.40
Pump	0.08	0.27	0.08	0.26	0.14	0.44	0.14	0.44	0.19	0.62	0.19	0.62	0.25	0.79	0.25	0.79
Total exergy destruction	692.84	617.18	894.43	767.25	877.15	835.31	1082.73	986.61	1071.44	1068.97	1281.13	1221.31	1263.28	1298.91	1474.98	1448.29
Exergy supply from fuel	1061.69	916.53	1593.64	1474.08	1265.01	1196.77	1855.83	1833.41	1464.51	1472.41	2112.32	2184.25	1661.73	1744.24	2364.39	2526.45
Exergy supply from solar	101.99	197.22	0	103.47	253.84	368.89	145.89	269.11	419.72	561.76	308.66	459.39	585.39	754.52	471.42	650.03
Total exergy supply	1163.68	1113.75	1593.64	1577.54	1518.85	1565.67	2001.72	2102.52	1884.23	2034.17	2420.98	2643.63	2247.13	2498.76	2835.80	3176.47
Exergy recovered	465.15	490.84	692.82	804.68	636.05	724.69	913.45	1110.37	807.17	959.59	1134.37	1416.85	978.27	1194.28	1355.39	1722.78
Exergetic solar fraction (%)	8.8	17.7	0	6.6	16.7	23.6	7.3	12.8	22.3	27.6	12.7	17.4	26.1	30.2	16.6	20.5
Exergy loss																
Stack exhaust gas	9.45	9.5	9.28	9.32	9.39	9.41	9.2	9.2	9.32	9.32	9.11	9.1	9.26	9.23	9.03	8.98
Condenser cooling air	105.37	118.04	128.17	135.72	185.05	183.83	196.95	196.66	270.59	270.95	284.16	285.91	357.43	359.4	372.55	376.41
Total exergy loss	114.82	127.54	137.45	145.04	194.44	193.24	206.15	205.86	279.91	280.27	293.27	295.01	366.69	368.63	381.58	385.39

Table 5
Results of exergy destruction percentage for solar STIG cycle components and exergy loss (various PR, TIT and SAR).

Exergy destruction (%)	SAR = 0.3				SAR = 0.5				SAR = 0.7				SAR = 0.9			
	TIT = 900 °C		TIT = 1200 °C		TIT = 900 °C		TIT = 1200 °C		TIT = 900 °C		TIT = 1200 °C		TIT = 900 °C		TIT = 1200 °C	
	PR 10	PR 30	PR 10	PR 30	PR 10	PR 30	PR 10	PR 30	PR 10	PR 30	PR 10	PR 30	PR 10	PR 30	PR 10	PR 30
Compressor	3.47	5.05	2.69	4.06	2.74	3.73	2.22	3.16	2.25	2.92	1.88	2.55	1.91	2.40	1.63	2.08
Combustor	63.23	61.00	60.89	62.66	59.54	58.85	57.98	60.19	55.90	55.93	54.88	57.03	53.12	53.76	52.36	54.52
Turbine	4.99	9.58	3.86	7.65	4.76	8.54	3.85	7.17	4.57	7.82	3.81	6.78	4.45	7.38	3.79	6.55
Super heater (SH)	2.89	1.11	4.12	2.15	3.24	1.16	5.02	2.46	3.35	1.16	5.39	2.53	3.37	1.16	5.55	2.54
Economiser (ECO)	7.28	3.17	12.98	5.61	5.54	2.51	10.06	4.18	5.10	3.23	8.66	4.34	4.83	3.57	7.73	4.47
HRSG (SH + ECO)	10.17	4.27	17.10	7.77	8.78	3.67	15.07	6.63	8.45	4.39	14.05	6.87	8.19	4.73	13.28	7.00
Solar evaporator	0.08	0.02	0.13	0.07	0.05	0	0.10	0.05	0.03	0	0.07	0.02	0.01	0.08	0.05	0.01
Condenser	18.04	20.03	15.32	17.75	24.11	25.15	20.76	22.75	28.79	28.89	25.30	26.69	32.31	31.59	28.87	29.71
Pump	0.01	0.04	0.01	0.03	0.02	0.05	0.01	0.04	0.02	0.06	0.02	0.05	0.02	0.06	0.02	0.05
Total exergy destruction	100	100	100	100	100	100	100	100	100	100	100	100	100	100	100	100
% of Wasted exergy in the total exergy supply	0.49	0.51	0.35	0.36	0.37	0.36	0.28	0.26	0.30	0.28	0.23	0.21	0.25	0.22	0.19	0.17
Exergy loss																
% of Total exergy loss in the total exergy supply	9.9	11.5	8.6	9.2	12.8	12.3	10.3	9.8	14.9	13.8	12.1	11.2	16.3	14.8	13.5	12.1

Table 6
Results of exergetic efficiency in solar STIG cycle and its components (various PR, TIT and SAR).

Exergetic efficiency (%)	SAR = 0.3				SAR = 0.5				SAR = 0.7				SAR = 0.9			
	TIT = 900 °C		TIT = 1200 °C		TIT = 900 °C		TIT = 1200 °C		TIT = 900 °C		TIT = 1200 °C		TIT = 900 °C		TIT = 1200 °C	
	PR 10	PR 30	PR 10	PR 30	PR 10	PR 30	PR 10	PR 30	PR 10	PR 30	PR 10	PR 30	PR 10	PR 30	PR 10	PR 30
Compressor	92.4	94.4	92.4	94.4	92.4	94.4	92.4	94.4	92.4	94.4	92.4	94.4	92.4	94.4	92.4	94.1
Combustor	74.5	78.9	76.8	80.1	76.0	78.7	78.5	80.6	77.2	78.8	79.9	81.2	78.1	79.0	81.0	81.8
Turbine	95.8	94.7	96.7	95.9	95.9	94.8	96.8	96.0	95.9	94.8	96.8	96.0	95.9	94.9	96.8	96.0
Super heater (SH)	97.2	98.9	96.4	98.0	97.4	99.0	96.3	98.1	97.5	99.1	96.4	98.2	97.7	99.1	96.5	98.3
Economiser (ECO)	85.3	92.6	77.9	89.0	89.3	94.6	82.9	92.1	90.4	93.3	85.2	91.9	91.1	92.8	86.9	91.8
HRSG (SH + ECO)	90.3	95.7	85.0	92.8	93.0	96.9	88.9	94.8	93.8	96.5	90.6	95.0	94.4	96.4	91.7	95.2
Solar evaporator	99.8	100.0	99.6	99.8	99.9	100.0	99.8	99.9	100.0	100.0	99.9	100.0	100.0	99.9	99.9	100.0
Condenser	5.4	5.4	4.9	4.9	3.6	3.7	3.4	3.4	2.8	2.8	2.7	2.7	2.3	2.3	2.3	2.2
Pump	81.6	81.6	81.6	81.6	81.6	81.6	81.6	81.6	81.6	81.6	81.6	81.6	81.6	81.6	81.6	81.6
Cycle exergetic efficiency	40.0	44.1	43.5	51.0	41.9	46.3	45.6	52.8	42.8	47.2	46.8	53.6	43.5	47.8	47.8	54.2

exergy loss and exergetic efficiency of each component in the cycle are also shown in Table 5 and Table 6 respectively. These results denote the usefulness of each component in the solar hybrid STIG cycle.

5.1. Solar STIG cycle

The total exergy destruction in the cycle increases with SAR. At a given TIT, a higher PR decreases the total exergy destruction and at a given PR, a higher TIT increases the total exergy destruction in the cycle. But, it is beneficial that the exergy recovered increases with PR, TIT and SAR. At a given PR, a higher TIT improvement of exergy recovery is higher. The exergy destruction in the solar STIG cycle for four real gas turbines, mentioned in Table 2, increases with SAR is shown in Fig. 4. The cycle exergy destruction is higher in the case D due to high TIT. At a given SAR, higher exergy destruction magnitudes are recorded in the combustor and condenser with high TIT.

Similarly, the exergetic efficiency also increases with SAR due to the increment in exergy recovery. For the given SAR, the exergetic efficiency is higher at high PR and TIT. At PR = 30, SAR = 0.3, the percentage increment of exergy recovery is 71.5%, when TIT varies from 900 °C to 1200 °C. The effect of SAR on exergetic efficiency of the solar STIG cycle for the four combinations of PR and TIT is shown in Fig. 5. It is beneficial that the exergetic efficiency of solar STIG cycle increases with SAR. The greater exergetic efficiency is obtained at SAR = 0.7, in the case D about 54.4%, and the percentage variation is 5.8%.

The exergetic solar fraction increases with SAR and maximum value is recorded at higher PR and low TIT. Fig. 6 presents the exergetic solar fraction as a function of SAR. For all the cases the exergetic solar fraction increases with SAR, and it also increases

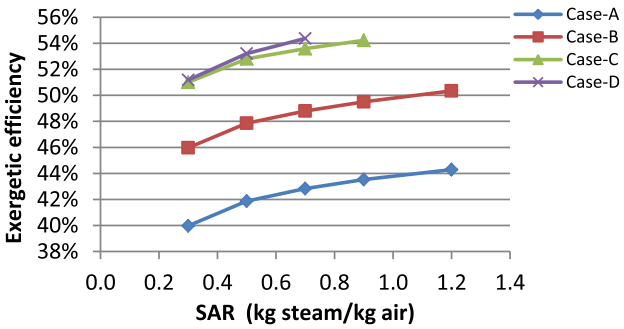

Fig. 5. Exergetic efficiency of Solar STIG cycle vs Steam to air ratio.

with decreasing PR and TIT. For case D, at SAR = 0.7, the paramount exergetic solar fraction about 11% is recorded.

Besides, the waste heat available in the turbine exhaust stream is sufficient to generate steam when SAR = 0.3 and therefore the exergetic solar fraction is null. The magnitude of exergy destruction in all components in the cycle (except compressor) increases by increasing SAR. It is suggested that the exergetic performance improves despite continuously increasing the total exergy destruction in the cycle.

The exergy destructions occur due to irreversibilities with in a component or system. The exergy loss occurs when the energy associated with a material or energy stream as stack gas and condenser outlet air is rejected to the environment. It is assumed in the analysis that the unused exergy of warm air at condenser exit is destroyed in the condenser. The total exergy loss increases only

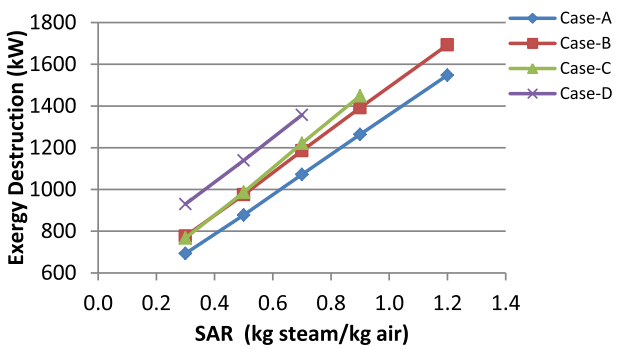

Fig. 4. Exergy destruction in solar STIG cycle vs steam to air ratio.

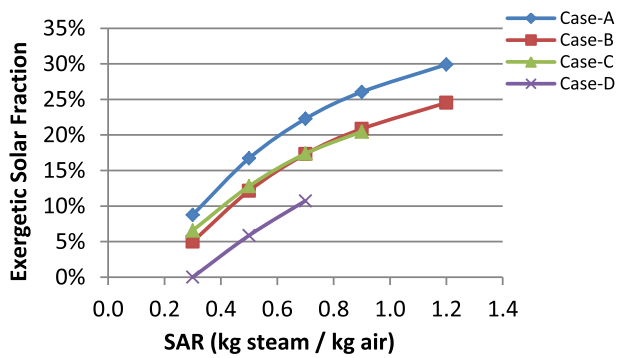

Fig. 6. Exergetic solar fraction of Solar STIG cycle vs Steam to air ratio.

Please cite this article in press as: Selwynraj AI, et al., Exergy analysis and annual exergetic performance evaluation of solar hybrid STIG (steam injected gas turbine) cycle for Indian conditions, Energy (2014), http://dx.doi.org/10.1016/j.energy.2014.12.001

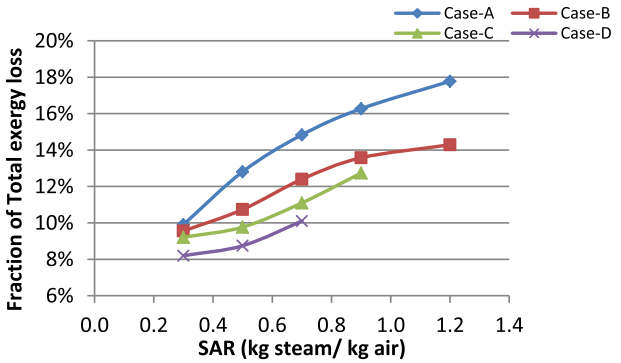

Fig. 7. Effect of SAR on total exergy loss of the solar STIG cycle.

Table 7
Exergetic performance of STIG and solar hybrid cycles.

Cycle	Exergetic efficiency	Solar fraction	Source
Integrated Bio gas-fuelled solid oxide fuel cell and STIG	42.2%–43.8%	–	[23]
Regenerative STIG	43.9%–45.6%	–	[8]
STIG based combined cycle	48.1%	–	[9]
STIG LM-2500 PE	52%	–	[16]
Combined cycle	54.3%	–	[24]
Integrated solar combined cycle	58.4%–60.9%	23.7%–27.8%	[24]
Advanced oxy-fuel hybrid power system (AHPS)	55.9%	59.9%	[25]
Solar tower/parabolic through with steam and organic turbine	24.5%–26%	100%	[26,27]

with SAR and depends on the temperature at which the heat is lost to the surroundings.

The fraction of total exergy loss of the solar hybrid STIG cycle is shown in Fig. 7. This value is higher in case A (PR = 10; TIT = 900 °C) due to lower cooling air outlet temperature.

The previous results of exergy analysis on STIG cycles and solar hybrids cycles are shown in Table 7.

The hybrid solar STIG cycle shows values of exergetic efficiency up to 54.4% (Fig. 5), a little lower than the maximum reported for the integrated solar combined cycle (ISCC). A possible explanation is that the ISCC has higher exergetic efficiency at the same solar fraction (based on energy) because the steam temperature provided by the solar collectors is higher, i.e., its solar input has higher exergetic value. But higher temperature demands more expensive solar collectors; therefore another comparison should be made on the economic basis which is outside the focus of this work. In Ref. [16] the case of LM 2500 PE gas turbine (PR = ~27 TIT = ~1150 °C) was evaluated at SAR_M (maximum steam generation without supplementary burning) and higher values. The exergetic efficiency at SAR_M shows similar results to case D, which is the parametrically the closest to this turbine. However, the additional steam, that was generated using external burner, decreased the exergetic efficiency. This confirms that the utilization of solar heat for evaporation is more feasible. In order to understand the behaviour of each component in the cycle, percentage of exergy destruction and exergetic efficiency are found.

5.2. Compressor

The exergy destruction in the compressor increases with compressor pressure ratio and does not depend on SAR and TIT (Table 4). Since steam is injected beyond the compressor, it will not affect the compressor performance. Sanjay [28] described that the exergy destruction in compressor is more at higher PR due to higher power consumption and increased bleeding of coolant air. The percentage of exergy destruction slightly decreases when increasing values of PR, TIT and SAR (Table 5). The exergetic efficiency of the compressor is almost constant about 94% at PR = 30 and 92% at PR = 10 (Table 6).

5.3. Combustor

As expected the combustion chamber is the most destructive component in the cycle, and the magnitude of exergy destruction increases with SAR and TIT. George Tsatsaronis et al. [29] expressed that the irreversibilities are due to the chemical reactions inside the combustion chamber, fluid friction by injecting large quantities of steam as well as high temperature difference between the operating fluid and flame and also, due to mixing of steam and gas in the combustor. As mentioned earlier the lower PR and TIT demands more solar exergy due to lower turbine outlet temperature which leads to lower exergy destruction in the combustor (Table 4). In the case of SAR = 0.7, at a given TIT, exergy destruction in the combustor variation is almost nil (PR = 10; TIT = 900 °C) with the PR and increases largely with increasing TIT. The reason being, beyond SAR = 0.5, at high PR, exergy of compressed air being supplied to the combustion chamber will not help in reducing the fuel consumption. The exergy supply from both fuel and solar is increased to achieve a huge quantity of super heated steam to the required TIT. I.O.Marrero et al. [30] also obtained the aforementioned outcome of the effect of steam injection on combustor from the exergy analysis of Brayton gas topping cycle in a combined triple power cycle by varying TIT, PR, and amount of steam injection.

In solar STIG cycle, the performance of the combustion chamber improves with SAR, because the rate of increment in the exergy supply from fuel surpasses the rate of increase of exergy destruction in the combustor. The percentage of exergy destruction in the combustor decreases from 63.2% to 52.4% (Table 5), and the exergetic efficiency of combustor increases from 74.5% to 81.8% (Table 6) with increasing SAR from 0.3 to 0.9. Moreover, by improving SAR, the exergy destructions of HRSG and condenser contribute more to the cycle. Fig. 8 shows the effect of steam to air ratio on the exergetic performance of the combustion chamber. The rate of exergy destruction in the combustor increases with SAR and TIT. Though the magnitude of exergy destruction in the combustor is more in the case D (PR = 20; TIT = 1400 °C), the fraction of exergy destruction in the combustor is less. However, the higher TIT requires elevated fuel exergy supply. This fraction denotes the effectiveness of the device. It indicates the portion of

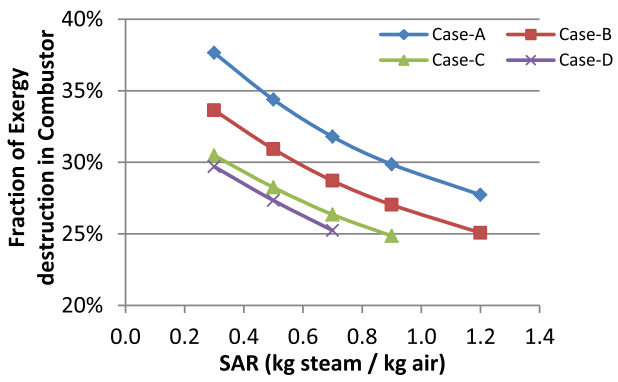

Fig. 8. Effect of SAR on exergetic performance of the combustor.

Please cite this article in press as: Selwynraj AI, et al., Exergy analysis and annual exergetic performance evaluation of solar hybrid STIG (steam injected gas turbine) cycle for Indian conditions, Energy (2014), http://dx.doi.org/10.1016/j.energy.2014.12.001

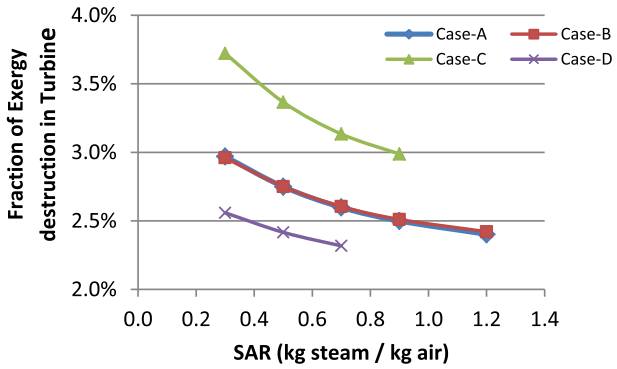

Fig. 9. Effect of SAR on exergetic performance of the Turbine.

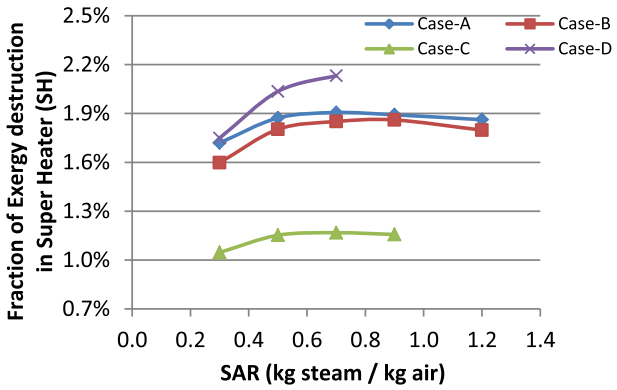

Fig. 10. Effect of SAR on exergetic performance of the super heater (SH).

exergy destroyed from the total exergy supplied to the solar STIG cycle.

5.4. Turbine

The exergy destruction in the turbine increases with compressor pressure ratio, SAR and independent of TIT (Table 4). The turbine experiences more exergy destruction at a higher PR due to higher expansion ratio which leads to more entropy generation. Increasing SAR enhances the total mass flow through the turbine and with it the fluid friction, therefore exergy destruction in the turbine increases with SAR. The percentage of exergy destruction in the turbine, at varying PR = 10–30 and TIT = 900 °C–1200 °C, decreases in the range of 9.6%–3.8% (Table 5), and exergetic efficiency is almost constant about 96% (Table 6) with increasing SAR from 0.3 to 0.9. Fig. 9 presents the effect of SAR on exergetic performance of the turbine. Similarly, in the case D, the fraction of exergy destruction in the turbine is lower than other cases as a result of higher exergy supply. As described in the case C (PR = 30; TIT = 1200 °C), higher fraction of exergy destruction is recorded in the turbine owing to higher pressure (expansion) ratio.

5.5. HRSG (SH (super heater) + ECO (economiser)) and solar evaporator

The heat recovery steam generator (HRSG) consists of super heater and economiser. The exergy destruction in the HRSG increases with SAR (Table 4). As stated before, at a given TIT, a higher pressure ratio will demand more solar share caused by higher expansion ratio in the turbine which leads to lower turbine outlet temperature and thereby reduces the irreversibilities in the HRSG. The exergy destruction in the super heater (SH) is less compared to the economiser in the HRSG, because the heat energy available in the turbine exhaust stream is primarily used for super heating the steam. But in the case of economiser, the exergy destruction slightly decreases when the SAR = 0.5 and then increases with SAR. At SAR = 0.5, the percentage increment of solar contribution is high over a range of PR and TIT while comparing with other SAR values presented in the Table 4. The exergy destruction in the solar evaporator increases with least magnitude with increasing SAR. At a given TIT, a higher pressure ratio decreases the exergy destruction in the solar evaporator. The percentage of exergy destruction in the HRSG, at varying PR = 10–30 and TIT = 900 °C–1200 °C, decreases in the range of 17.1%–3.7% and exergetic efficiency increases in the range of 85%–97% with increasing SAR from 0.3 to 0.9. This requires high performance heat recovery systems. The percentage of exergy destruction in the solar evaporator is less than 0.1%, and the exergetic efficiency is almost 100%, because heat derived from solar field is predominantly used for evaporation, and the temperature difference is much less induced by pressure drop in the evaporator (Tables 4 and 6).

Fig. 10 and Fig. 11 depict the exergetic performance of super heater (SH), economiser (ECO), over a range of SAR. The effect of SAR on exergetic performance of HRSG (combination of SH and ECO) is illustrated in Fig. 12. The fraction of exergy destruction in the HRSG records highest value of 7.1% in the case D due to the requirement of high temperature superheated steam corresponds to high TIT and lower value of 3.1% in the case C as a result of high expansion ratio in the turbine. In solar STIG cycle, the temperature of the super heated steam to be injected into combustor relies upon

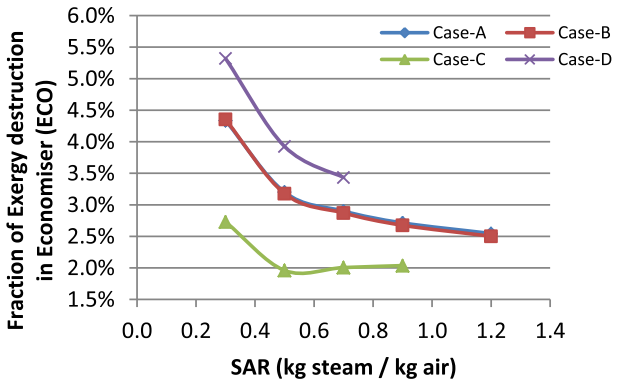

Fig. 11. Effect of SAR on exergetic performance of the Economiser (ECO).

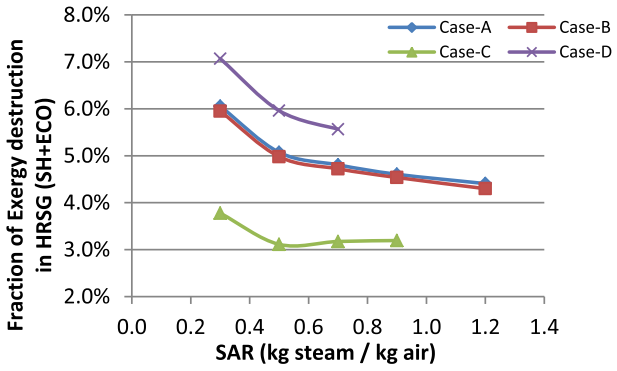

Fig. 12. Effect of SAR on exergetic performance of the HRSG (SH + ECO).

Please cite this article in press as: Selwynraj AI, et al., Exergy analysis and annual exergetic performance evaluation of solar hybrid STIG (steam injected gas turbine) cycle for Indian conditions, Energy (2014), http://dx.doi.org/10.1016/j.energy.2014.12.001

the PR, TIT, SAR and pinch point in the HRSG. Irreversibility in the heat exchanger is caused principally by the heat transfer over a finite temperature difference.

The exergy destruction in the economiser for all the cases slightly decreases up to the SAR = 0.5 due to lower value of LMTD (log mean temperature difference) and then increases with SAR. But, in all cases mentioned in the Table 2, the larger heat exchanger area is required for the SAR = 0.5 which leads to higher cost of economiser while comparing with other SAR values of 0.3, 0.7, 0.9, except SAR = 1.2 in the case B.

5.6. Condenser, pump and stack

The amount of water vapour present in the exhaust stream depends heavily on the injected steam into the combustor and water vapour formed during the oxidation of fuel. The condenser is required to recover the water and reuse to the cycle. Otherwise it would be lost to the surroundings and not to recuperate exergy. As the SAR increases, the exergy destruction in the condenser increases due to increased condensation. At a given SAR, the exergy destruction in the condenser increases only with TIT irrespective of the pressure ratio, since the condensation takes place at atmospheric pressure and large quantity of heat is removed from the condenser by cooling air supplied by condenser fans. The percentage of exergy destruction in the condenser, at varying PR = 10–30 and TIT = 900 °C–1200 °C, increases in the range of 15.3%–32.3% and exergetic efficiency decreases in the range of 5.4%–2.2% with increasing SAR from 0.3 to 0.9.

The sole purpose of condenser is to recover the water for recycling. The fraction of exergy destruction in condenser for four cases at various SAR values is shown in Fig. 13. The fraction of exergy destruction in the condenser is lower in case D (PR = 20; TIT = 1400 °C), due to higher fuel exergy and increases with SAR being large amount of heat rejection. The exergy loss in the condenser is due to the heat lost to the surroundings by cooling air, and it increases with SAR but decreases with increasing outlet air temperature. The outlet temperature of cooling air was determined from equation (12). After capturing water from the exhaust gas, the little magnitude of exergy is not only lost or wasted but also dispose the thermal pollution into the environment. The exergy loss in the stack is almost constant regardless of TIT, PR and SAR due to constant exhaust gas temperature. It is well known that the exergy loss in the stack at lower temperature results in efficient heat recovery steam generation system and reduces the irreversibilities in the combustor. The exergy destruction in the pump increases with PR and SAR and does not depend on TIT. As the SAR increases, the exergy destruction in the pump increases due to fluid friction. The percentage of exergy destruction in the pump and exergy loss in the stack is less than 1%. The exergetic efficiency of stack is null, because it is used only to expel the low temperature flue gas to the atmosphere which has no work potential to be utilized to improve the plant performance. The exergetic efficiency of the pump is constant about 81.6% regardless of the PR, TIT and SAR, since the pump is employed to feed the water to the HRSG matching with compressor exit pressure.

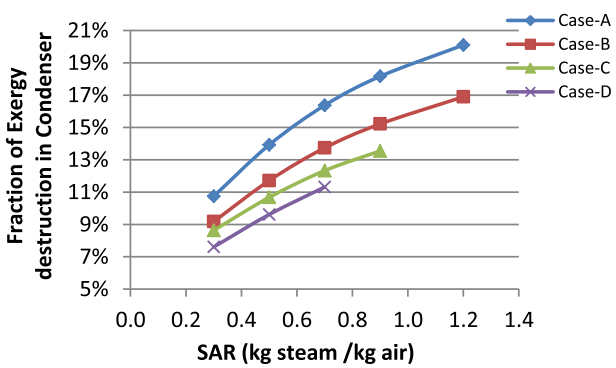

Fig. 13. Effect of SAR on exergetic performance of the Condenser.

6. Annual performance results

Two modes of operation were considered, CP (constant power output) and VP (variable power output). Constant power mode maintains constant SAR through the turbine and constant power output. Therefore whenever there is not enough solar power, duct firing is added after the HRSG in order to generate the required SAR. As described by T.S. Kim and S.H. Hwang [31], to enhance part load efficiency, high turbine exhaust temperature is maintained for each SAR values in VP mode of operation.

6.1. Constant power results

Fig. 14 illustrates the variations of exergetic efficiency for the span of the day right through the year for Indore and Jaipur in constant power mode. The variations are analogous to the corresponding DNI distribution pattern for the respective locations. The ambient temperature and relative humidity have a small effect on the exergetic performance of the solar hybrid STIG cycle. The low DNI and high surrounding temperature during the summer months lead to low exergetic efficiency. At the beginning as well as the end of the year, the exergetic performance of the cycle is favourable due to high DNI and low ambient temperature. Since

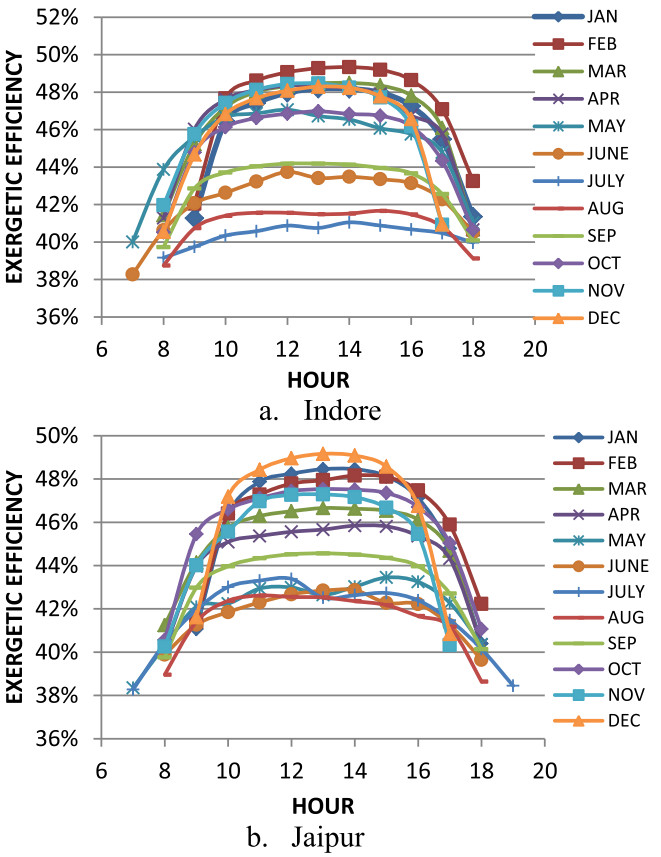

Fig. 14. Annual variation of exergetic efficiency, constant power mode, for SAR = 0.7.

Please cite this article in press as: Selwynraj AI, et al., Exergy analysis and annual exergetic performance evaluation of solar hybrid STIG (steam injected gas turbine) cycle for Indian conditions, Energy (2014), http://dx.doi.org/10.1016/j.energy.2014.12.001

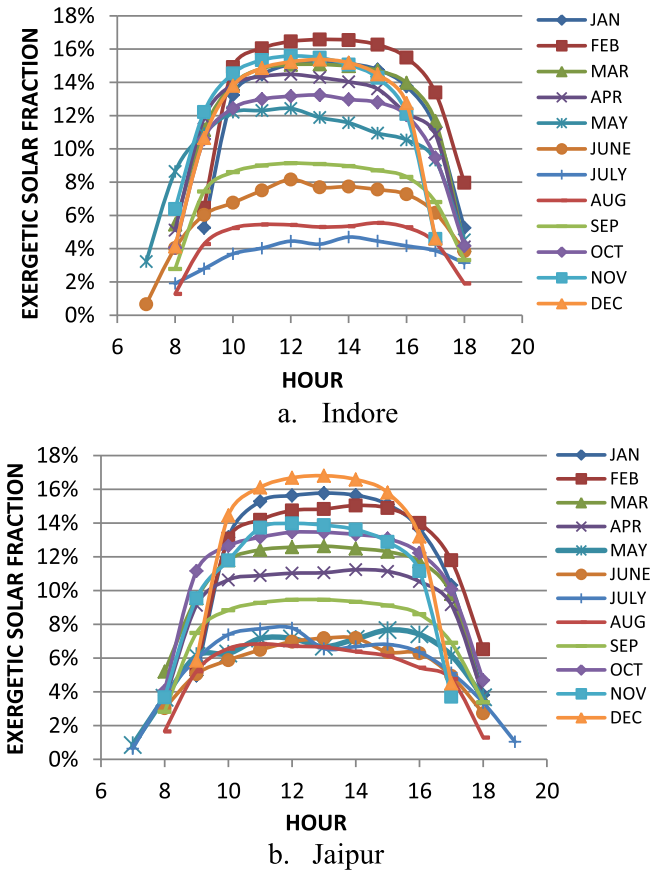

Fig. 15. Annual variation of exergetic solar fraction, constant power mode, for SAR = 0.7.

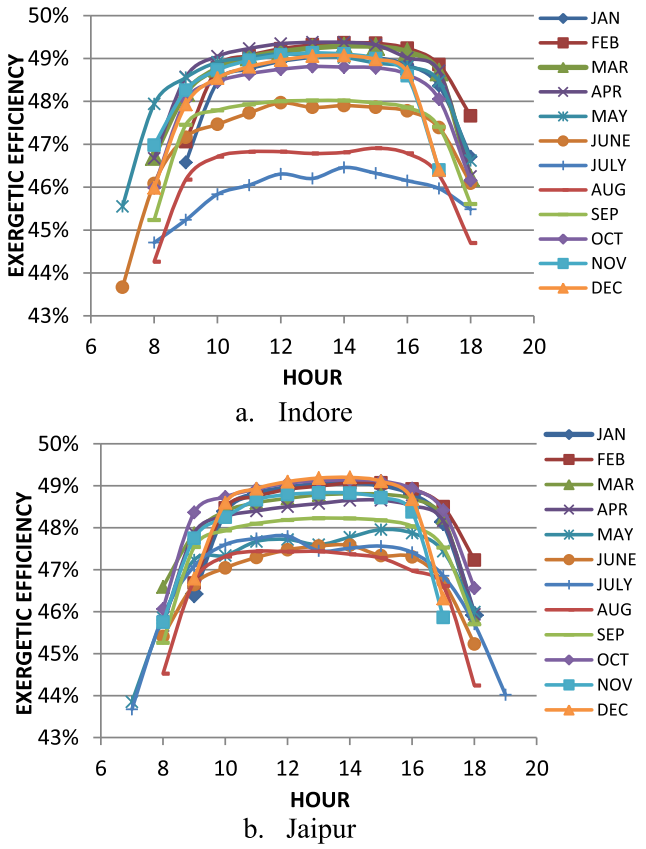

Fig. 16. Annual variation of exergetic efficiency, variable power mode, for SAR = 0.7.

the temperature of air inlet and fuel are equal, the exergy of fuel decreases with increasing ambient temperature. Moreover, the exergy destruction in the condenser also decreases at higher ambient temperature and hence, exergetic performance of the solar STIG cycle is improved.

However, during the peak sun shine hours (10 am–4 pm), the effect of DNI prevails over the surrounding temperature and relative humidity of inlet air. The hourly variation of exergetic solar fraction shown in Fig. 15 also confirms that the cycle exergetic efficiency improves when the solar share rises and it also follows the annual DNI variation. Table 8 displays the constant power exergetic performance results for the locations; Indore and Jaipur. Owing to high plant operational hours, with moderate insolation, the exergetic performance of Jaipur is lesser than Indore. The annual electric power generation capacity ranges from 1.664×10^3 MWh_e to 4.241×10^3 MWh_e for Indore and 1.583×10^3 MWh_e to 4.444×10^3 MWh_e for Jaipur over the range of SAR mentioned in Table 8. Adding duct firing for maintaining constant power supply during low insolation hours will increase the exergy destruction. The smallest area of the solar collector was determined for each location based on peak DNI value corresponding to produce same SAR in both constant and variable power scenarios. Due to more DNI fluctuation and the size of the collector, the exergy of fuel from duct firing increment is more in Jaipur than Indore which leads to lower exergetic solar fraction. Moreover, it is not considered to operate the solar STIG plant when the hourly DNI is less than 300 W/m^2 around the year due to its unfavourable solar to electricity efficiency.

The exergetic efficiency increment is very small due to high operating hours in Jaipur for SAR 0.5 than SAR 0.7. For the same SAR value, the power output of solar STIG plant is less in Indore than Jaipur due to larger number of operational hours with moderate insolation and their size of solar field. Further increasing the size of

Table 8
Annual exergetic performance results for constant power mode at Indore and Jaipur.

Indore						Jaipur				
SAR	0.3	0.5	0.7	0.9	1.2	0.3	0.5	0.7	0.9	1.2
E_{fuel} (MWh_{th}) x10^3	3.446	4.159	4.701	5.366	6.342	3.281	4.362	5.020	5.664	6.664
$E_{duct\ firing}$ (MWh_{th}) x10^3	0.104	0.331	0.53	0.76	1.099	0.125	0.478	0.815	1.138	1.62
E_{solar} (MWh_{th}) x10^3	0.137	0.429	0.743	1.064	1.546	0.122	0.406	0.709	1.009	1.46
Power (MWh_e) x10^3	1.663	2.264	2.777	3.363	4.241	1.583	2.374	2.966	3.55	4.444
η_{II} (%)	45.1	46.0	46.5	46.8	47.2	44.9	45.27	45.32	45.5	45.7
Operational hours	2589	2589	2506	2506	2506	2464	2715	2676	2645	2625
SF_{II} (%)	3.7	8.7	12.4	14.8	17.2	3.5	7.7	10.8	12.9	15.0
$A_{solar\ collector}$ (m^2/kg -air)	336.17	1054.45	1856.0	2658.01	3862.03	264.0	931.93	1643.41	2354.39	3421.83

Please cite this article in press as: Selwynraj AI, et al., Exergy analysis and annual exergetic performance evaluation of solar hybrid STIG (steam injected gas turbine) cycle for Indian conditions, Energy (2014), http://dx.doi.org/10.1016/j.energy.2014.12.001

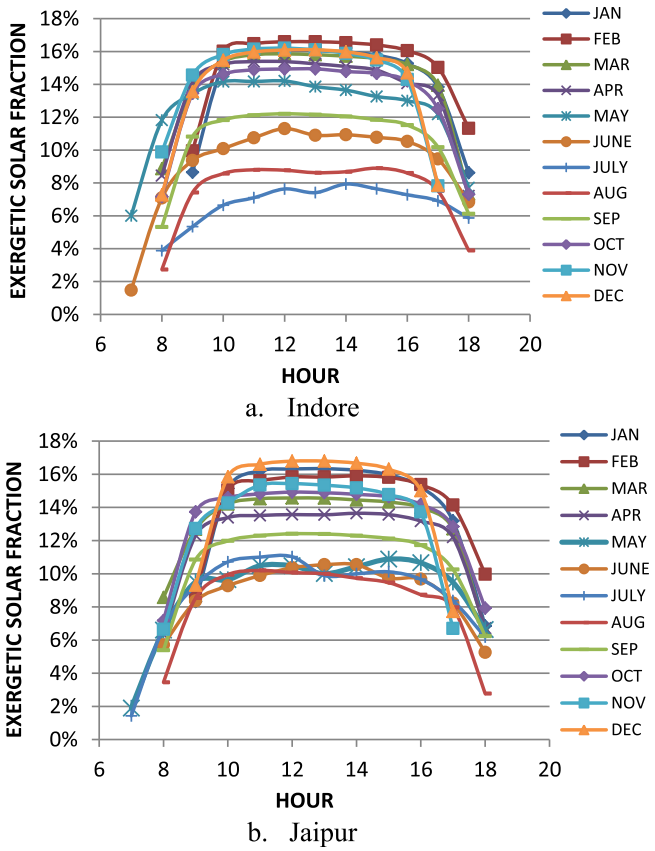

Fig. 17. Annual variation of exergetic solar fraction, variable power mode, for SAR = 0.7.

the solar collector requires thermal (latent heat) storage system to store heat beyond requirement only at peak DNI which demands more capital cost than duct firing. However, incorporating thermal storage system enhances the solar fraction and plant operational hours with solar energy.

6.2. Variable power results

In the variable power scenario, the power output of the cycle varies to follow the solar radiation. Since the SAR depends on available DNI, the turbine isentropic efficiency changes according to the varying actual mass flow rate through the turbine during the operation. The effect of ambient temperature in variable power mode is suppressed by the actual steam generated based on available DNI. The variations of exergetic efficiency and exergetic solar fraction for the span of the day around the year for Indore and Jaipur in variable power mode are shown in Fig. 16 and Fig. 17 respectively. The variation is similar fashion in constant power mode.

The results from the Table 9 show the annual exergetic performance of solar STIG cycle at Indore and Jaipur in variable power mode. Since there is no supplementary duct firing and higher plant operating hours, the exergetic solar fraction and exergetic efficiency are high compared to constant power mode.

But, the exergetic efficiency during peak sun shine hours is very similar in both scenarios due to high solar insolation. The annual electric power output is also slightly high in the range of 1.737×10^3 MWh_e to 4.33×10^3 MWh_e for Indore and 1.744×10^3 MWh_e to 4.234×10^3 MWh_e for Jaipur.

7. Conclusions

The exergetic performance of solar hybrid STIG cycle under nominal conditions and the annual exergetic performance using typical meteorological year data for Indore and Jaipur are presented. It is found from the results that the steam injection does not affect the performance of compressor. The exergy destruction in the compressor marginally increases with compressor pressure ratio and does not depend on SAR and TIT. The combustion chamber is the most destructive component in the cycle, and the magnitude of exergy destruction increases with SAR and TIT. The performance of the combustion chamber improves with SAR, because the rate of increment in the exergy supply from fuel surpasses the rate of increase of exergy destruction in the combustor. But it has to be well designed for stable operation in the presence of high SAR. The exergetic efficiency of combustor increases from 74.5% to 81.8% with increasing SAR from 0.3 to 0.9. The turbine experiences more exergy destruction at a higher PR due to higher expansion ratio which leads to more entropy generation. The exergy destruction in the turbine is independent of TIT and increases with SAR, and the percentage of increment decreases from 17.2% to 12.7% over the range of SAR 0.3–0.9.

The exergy destruction in the HRSG increases with SAR. The exergy destruction in the super heater (SH) is less compared to the economiser in the HRSG. At a given SAR and low PR, the exergy destruction in HRSG significantly increases with higher TIT due to more heat recovery which causes large temperature difference in the economiser. As a result, the contribution of solar heat (exergetic solar fraction) is more sensitive to TIT and SAR than PR. Generally, the exergetic efficiency improves as the exergetic solar fraction is increased. Higher pressure and temperature in the solar field will improve the exergetic efficiency and thereby, increases the cost based on PR and TIT. The exergetic efficiency of HRSG increases in the range of 85%–97% with increasing SAR from 0.3 to 0.9. This requires high performance heat recovery systems. The percentage of exergy destruction in the solar evaporator is less than 0.1% due to collected heat from solar field is predominantly used for evaporation. The exergy destruction in the condenser increases mainly

Table 9
Annual exergetic performance results for variable power mode at Indore and Jaipur.

Indore						Jaipur				
SAR	0.3	0.5	0.7	0.9	1.2	0.3	0.5	0.7	0.9	1.2
E_{fuel} (MWh_{th}) $\times 10^3$	3.663	4.853	5.481	6.078	6.941	3.699	4.944	5.543	6.105	6.914
E_{solar} (MWh_{th}) $\times 10^3$	0.143	0.476	0.838	1.2	1.744	0.133	0.449	0.791	1.133	1.647
Power (MWh_e) $\times 10^3$	1.737	2.517	3.015	3.569	4.33	1.744	2.534	3.042	3.526	4.234
η_{II} (%)	45.6	47.2	48.3	49.0	49.9	45.5	47.0	48.0	48.7	49.5
Operational hours	2810	3236	3236	3236	3236	2858	3352	3352	3352	3352
SF_{II} (%)	3.8	8.9	13.3	16.5	20.1	3.5	8.3	12.5	15.7	19.2
$A_{solar\ collector}$ (m^2/kg-air)	336.17	1054.45	1856.0	2658.01	3862.03	264.0	931.93	1643.41	2354.39	3421.83

Please cite this article in press as: Selwynraj AI, et al., Exergy analysis and annual exergetic performance evaluation of solar hybrid STIG (steam injected gas turbine) cycle for Indian conditions, Energy (2014), http://dx.doi.org/10.1016/j.energy.2014.12.001

with SAR and TIT. The second largest percentage of exergy destruction in the flue gas condenser is to recover water for recycling, and the exergy loss increases linearly with SAR due to heat removal from the condenser is lost to the surroundings by cooling air. This requires large size of air cooled condenser which increases capital cost of the solar STIG plant. Further study is required to find the low cost air cooled condenser. The exergetic efficiency of flue gas condenser decreases from 5.4% to 2.2% as the SAR increases. Moreover, the constant magnitude of dry flue gas exergy also lost to the surroundings regardless of TIT, PR and SAR. The percentage of exergy destruction in the pump and exergy loss in the stack exhaust gas is less than 1%. The exergetic efficiency of the pump is constant about 81.6% regardless of the PR, TIT and SAR. The total exergy destruction in the cycle increases with SAR and TIT. The exergetic efficiency of the solar STIG cycle also increases in the range of 40%–54.2% with SAR up to 0.9, indicating the efficient usage of the available thermodynamic resources. The hybridization enables 'raising' the quality of conversion of the solar heat, which by itself would not be able to reach these high conversion efficiencies. The magnitude of exergy destruction in all components in the cycle (except compressor) increases by increasing SAR.

The annual exergetic solar fraction ranges between 3.7 and 17.2% for constant power scenario and 3.8–20.1% for variable power scenario over the range of SAR values. The annual exergetic efficiency reaches 49.9% at higher SAR in variable power scenario and 47.2% in constant power scenario at higher SAR. Increasing the exergetic solar fraction increases the performance of the solar STIG cycle. Higher SAR value during the year will increase the exergetic efficiency since it enables higher solar participation, it will also increase the net power output of the cycle. The annual values of exergetic solar fraction and exergetic efficiency at Indore are higher than Jaipur in both constant and variable power modes of operation. Further detailed financial analysis of solar hybrid STIG plant is necessary and comparable with other solar thermal based plants. In order to find the optimum location, the presented annual exergetic performance results and annual energy performance results from past work will be helpful to carryout the cost analysis for Indore and Jaipur.

Acknowledgement

The authors acknowledge the financial support provided by the Ministry of Science and Technology, Government of India (Sanction no: DST/INT/ISR/P-7/ 2011), and the Ministry of Science and Technology, Israel, for Indo-Israel collaborative project.

Nomenclature

BIG/STIG	biomass integrated gasification/steam injected gas turbine
C	velocity
CP	constant power
DNI	direct normal irradiance, W/m^2
dT	temperature difference, °C
e	specific exergy, kJ/kg
ECO	economiser
$\dot{E}$	exergy rate, kW
g	gravitational acceleration, m/s^2
GENSET	gas turbine generation set
h	specific enthalpy, kJ/kg
$\overline{h}$	specific molar enthalpy, kJ/kg.mol
HRSG	heat recovery steam generator
IAC	inlet air cooling
$\dot{m}$	mass flow rate, kg/s
P	pressure
PR	pressure ratio
$\dot{Q}$	heat transfer rate, kW
$\overline{R}$	universal gas constant (8.314 kJ/kgmol.K)
RW	recycle water
s	specific entropy kJ/kg.K
$\overline{s}$	specific molar entropy kJ/kg mol.K
SAR	steam to air ratio, kg-steam/kg-air
SF	solar fraction
SH	super heater
T	temperature, °C or K
TIT	turbine inlet temperature, °C
VP	variable power
$\dot{W}$	work rate, kW per kg-air/s (or) specific work, kJ/kg-air
x	mole fraction
z	altitude, m

Sub- and super- scripts

0	environmental state
1–13	state points
C	compressor
ch	chemical
CH_4	methane
CO_2	carbon dioxide
D	condenser, destruction
e	electricity
H_2O	water
II	second law, exergetic
in/out	input/output
m	matter, MAXIMUM
N	net
O_2	oxygen
P	pump
ph	physical
Q	heat
sys	system
T	turbine
w	work

References

[1] Livshits M, Kribus A. Solar hybrid steam injection gas turbine (STIG) cycle. Sol Energy 2012;86:190–9.
[2] Moran MJ. Engineering thermodynamics. CRC Press LLC; 1999.
[3] Jonssona Maria, Jinyue Yan. Humidified gas turbines—a review of proposed and implemented cycles. Energy 2005;30:1013–78.
[4] Abam DPS, Moses NN. Computer simulation of a Gas turbine performance. version 1.0 Glob J Res Eng February 2011;11(1). ISSN: 0975–5861.
[5] Sahebi Yaser, Hasan Athari. Exergy analysis of gas turbine with fogging inlet cooling. In: 2nd International Conference on Mechanical and Electronics Engineering (ICMEE 2010), Vol. 2; 2010. p. 201–5.
[6] Layi Fagbenle R, Oguaka ABC, Olakoyejo OT. A thermodynamic analysis of a biogas-fired integrated gasification steam injected gas turbine (BIG/STIG) plant. Appl Therm Eng 2007;27:2220–5.
[7] Wang FJ, Chiou JS. Performance improvement for a simple cycle gas turbine GENSET – a retrofitting example. Appl Therm Eng 2002;22:1105–15.
[8] Wang FJ, Chiou JS. Integration of steam injection and inlet air cooling for a gas turbine generation system. Energy Convers Manag 2004;45:15–26.
[9] Srinivas T, . Gupta AVSSKS, Reddy BV. Sensitivity analysis of STIG based combined cycle with dual pressure HRSG. Int J Therm Sci 2008;47:1226–34.
[10] Yilmazoğlu Mustafa Zeki, Amirabedin Ehsan. Second law and sensitivity analysis of a combined cycle power plant in Turkey. J Therm Sci Technol 2011;31:41–50. ISSN 1300–3615.
[11] Motahar Sadegh, Alemrajabi Ali Akbar. Exergy based performance analysis of a solid oxide fuel cell and steam injected gas turbine hybrid power system. Int J Hydrogen Energy 2009;34:2396–407.
[12] Nishida Kousuke, Takagi Toshimi, Kinoshita Shinichi. Regenerative steam-injection gas-turbine systems. Appl Energy 2005;81:231–46.
[13] Mansouri Mohammad Tajik, Ahmadi Pouria, Kaviri Abdolsaeid Ganjeh, Mohd Jaafar Mohammad Nazri. Exergetic and economic evaluation of the effect of

HRSG configurations on the performance of combined cycle power plants. Energy Convers Manag 2012;58:47–58.
[14] Kaushik SC, Siva Reddy V, Tyagi SK. Energy and exergy analyses of thermal power plants: a review. Renew Sustain Energy Rev 2011;15:1857–72.
[15] Ahmadi Pouria, Dincer Ibrahim, Rosen Marc A. Exergy, exergoeconomic and environmental analyses and evolutionary algorithm based multi-objective optimization of combined cycle power plants. Energy 2011;36:5886–98.
[16] Guarinello Jr FlaÂvio, Cerqueira SeÂrgio AAG, Nebra Silvia A. Thermoeconomic evaluation of a gas turbine cogeneration system. Energy Convers Manag 2000;41:1191–200.
[17] Siva Reddy V, Kaushik SC, Tyagi SK. Exergetic analysis and performance evaluation of parabolic trough concentrating solar thermal power plant (PTCSTPP). Energy 2012;39:258–73.
[18] Livshits M, Kribus A. Solar STIG cycle annual analysis. In: ASME 6 Int. Conf. Energy Sustain. San Diego, USA: ASME; 2012. p. 255–61.
[19] Selwynraj AI, Iniyan S, Suganthi L, Polonsky G, Kribus A. Annual thermodynamic analysis of solar power with steam injection gas turbine (STIG) cycle for Indian conditions. In: ISES Sol. World Congr., Cancun; 2013.
[20] Polonsky Guy, Livshits Maya, Immanuel Selwynraj A, Iniyan S, Suganthi L, Kribus Abraham. Annual performance of the solar hybrid STIG cycle. Sol Energy 2014;107:278–91.
[21] Tyagi SK, Wang Shengwei, Singhal MK, Kaushik SC, Park SR. Exergy analysis and parametric study of concentrating type solar collectors. Int J Therm Sci 2007;46:1304–10.
[22] De Paepe M, Dick E. Technological and economical analysis of water recovery in steam injected gas turbines. Appl Therm Eng 2001;21:135–56.
[23] Mazzucco Andrea, Rokni Masoud. Thermo-economic analysis of a solid oxide fuel cell and steam injected gas turbine plant integrated with woodchips gasification. Energy 2014;76:114–29.
[24] Li Yuanyuan, Yang Yongping. Thermodynamic analysis of a novel integrated solar combined cycle. Appl Energy 2014;122:133–42.
[25] Gou Chenhua, Cai Ruixian, Hong Hui. A novel hybrid oxy-fuel power cycle utilizing solar thermal energy. Energy 2007;32:1707–14.
[26] Al-Sulaiman Fahad A. Exergy analysis of parabolic trough solar collectors integrated with combined steam and organic Rankine cycles. Energy Convers Manag 2014;77:441–9.
[27] Xu Chao, Wang Zhifeng, Li Xin, Sun Feihu. Energy and exergy analysis of solar power tower plants. Appl Therm Eng 2011;31:3904–13.
[28] Sanjay. Investigation of effect of variation of cycle parameters on thermodynamic performance of gas-steam combined cycle. Energy 2011;36:157–67.
[29] Tsatsaronis George, Morosuk Tatiana, Koch Daniela, Sorgenfrei Max. Understanding the thermodynamic inefficiencies in combustion processes. Energy 2013;62:3–11.
[30] Marrero IO, Lefsaker AM, Razani A, Kim KJ. Second law analysis and optimization of combined triple power cycle. Energy Convers Manag 2002;43:557–73.
[31] Kim TS, Hwang SH. Part load performance analysis of recuperated gas turbines considering engine configuration and operation strategy. Energy 2006;31:260–77.

Please cite this article in press as: Selwynraj AI, et al., Exergy analysis and annual exergetic performance evaluation of solar hybrid STIG (steam injected gas turbine) cycle for Indian conditions, Energy (2014), http://dx.doi.org/10.1016/j.energy.2014.12.001